

This work was written as part of one of the author's official duties as an Employee of the United States Government and is therefore a work of the United States Government. In accordance with 17 U.S.C. 105, no copyright protection is available for such works under U.S. Law. Access to this work was provided by the University of Maryland, Baltimore County (UMBC) ScholarWorks@UMBC digital repository on the Maryland Shared Open Access (MD-SOAR) platform.

Please provide feedback

Please support the ScholarWorks@UMBC repository by emailing [scholarworks-group@umbc.edu](mailto:scholarworks-group@umbc.edu) and telling us what having access to this work means to you and why it's important to you. Thank you.



# Transitioning the NASA SLR network to Event Timing Mode for reduced systematics, improved stability and data precision

Thomas Varghese<sup>1</sup> · Randall L. Ricklefs<sup>1</sup> · Erricos C. Pavlis<sup>2</sup> · Magdalena Kuzmicz-Cieslak<sup>2</sup> · Stephen M. Merkowitz<sup>3</sup>

Received: 1 March 2019 / Accepted: 12 November 2019 / Published online: 21 November 2019  
© Springer-Verlag GmbH Germany, part of Springer Nature 2019

## Abstract

NASA's legacy Satellite Laser Ranging (SLR) network produces about one-third of the global SLR data to support space geodesy. This network of globally distributed stations has been using Time Interval Units (TIU) for range measurements for the last 25+ years. To improve the reliability of the SLR network and satisfy the need for stable millimeter precision data, a phased replacement of the TIUs in the network with picosecond-precise Event Timer Modules was initiated in 2015. This scheme allowed the time of flight and laser transmit epoch measurement to one picosecond resolution. For a network with global scientific impact, transitioning to a new data generation metrological scheme requires significant data scrutiny and long-term science data validation. Any long-term testing/measurement has the potential to interrupt the station's daily operational data flow to the International Laser Ranging Service (ILRS) as the station under test will have to put its test data into quarantine. We have demonstrated a very effective way to test and implement the new device without removing the old hardware and without the need for the orbit analysis. This operationally noninvasive scheme performed concurrent test measurements enabling uninterrupted operational data flow to the users, while allowing simultaneous test data capture for short- and long-term systematics and stability analysis. Extensive analysis of the test data was performed by the NASA SLR engineering team and the ILRS Analysis Standing Committee, to uncover biases and any dependencies on the satellite ranges (for nonlinear scale issues). Multi-ETM comparison was also performed at two of the SLR stations through the interchange of hardware to establish the inter-device range biases and stability. Such benchmarked hardware was subsequently sent to the remaining stations to allow traceability and normalize the network performance. The range bias intercomparison performed using the multiyear SLR data analysis agreed well with the engineering changes, thus validating the approach to flush out station-specific ranging systematics affecting precise orbit determination. Such an improvement and rebalancing of the current network will allow an orderly transition of the current NASA SLR network operating at a maximum rate of 10 Hz to the NASA next generation Space Geodesy Satellite Laser Ranging (SGSLR) network operating at 2 kHz (McGarry et al. in *J Geod*, 2018. <https://doi.org/10.1007/s00190-018-1191-6>; Merkowitz et al. in *J Geod*, 2018. <https://doi.org/10.1007/s00190-018-1204-5>).

**Keywords** Satellite laser ranging · Event timer module · Time interval unit · NASA SLR network · Range bias

## 1 Introduction

The NASA SLR network has eight stations that are globally distributed in 4 continents and 2 islands in the Pacific

✉ Thomas Varghese  
tv@cybioms.com

- <sup>1</sup> NASA SLR Engineering/Cybioms Corporation, Rockville, MD 20850, USA
- <sup>2</sup> Joint Center for Earth Systems Technology (JCET), University of Maryland Baltimore County, Baltimore, MD 21250, USA
- <sup>3</sup> NASA Goddard Space Flight Center, Greenbelt, MD 20771, USA

and contributes approximately 30% of the total International Laser Ranging Service (ILRS) data. The space geodetic and Earth science communities desire millimeter-level data precision and stability from the SLR measurements to support the International Terrestrial Reference Frame (ITRF) (Altamimi et al. 2016) and precision orbit determination (POD) (Pearlman et al. 2019; Arnold et al. 2018) of Earth observing spacecraft (particularly altimetry missions). A critical part of the SLR measurement is the two-way time of flight (TOF) measurement, which was performed by the Hewlett Packard HP 5370 Time Interval Unit (TIU) in the NASA stations for more than 2 decades. This device has a number of performance limitations. The TIU performance is

limited to a time resolution of 20 picoseconds (ps), a ranging precision of  $> 20$  ps, and a stability of  $\pm 50$  ps. It is also not possible to measure the epoch time with the TIU, and hence, a coarse counter is used to measure the epoch time to a resolution of 200 ns. These SLR stations operate at a maximum rate of 10 Hz due to the limitations of the laser and the electronics. The maximum operational pulse repetition frequency (PRF) was further constrained by the real-time TIU data transfer rate of the IEEE 488 interface of  $\sim 50$  ms. This constraint has seriously restricted the data quantity by limiting the rate of laser operation to the LAGEOS satellite to 5 Hz, to the GNSS group of satellites to 4 Hz, and to GEO satellites to only 2 Hz. The above limitations restrict the satellite data severely by today's standards.

The stability of the TIU has degraded over the years, and data often show significant range differences of several millimeters on a moving average of 30 points. Figure 1 shows a comparison performed by two TIUs taking data concurrently during a critical benchmarking/colocation effort at the NASA MOBLAS 7 station. These concurrent data from the two TIUs represent the data from LEO satellites of various altitudes along with the corresponding ground calibration data (shown at beginning of the data set). The green line trend function shows the 30-point moving average (MA) of this residual data set. Each group of data is a separate LEO satellite pass, except at the beginning of the plot (within blue dotted lines), which shows the calibration comparison data on a ground target of  $\sim 170$  m. The data MA difference is  $\pm 2$  mm with a mean of  $< 1$  mm). The total duration of this data sample on LEO satellites was  $\sim 40$  min, with each satellite data seen as a separate group. As it can be seen, the satellite range difference between the two devices was as high as 9 mm for the 30-point MA. It also illustrates the variability

of the range difference within the same satellite pass. The data loop modules such as the detectors, signal processing hardware, timing, and frequency standard were common for both devices in this measurement. Therefore, the observed variation can only be solely attributed to the variability of the systematics in the two TIUs based on satellite ranges.

The TIU has shown jumps in the TOF data, sometimes approaching multiple centimeters. Such large jumps necessitate an immediate replacement of the device with an alternate one. These systematic range offsets cannot be quality controlled at the station without a global orbit analysis. Figure 2 illustrates a large jump ( $\sim 10$  cm) observed in the MOBLAS 7 TIU data from such a global fit, and the device had to be immediately replaced upon the anomaly confirmation. Very large jumps can be quickly determined from the daily QC process based on orbit analysis, while smaller ( $< 1$  cm) RB requires data analysis over a substantially longer period. To avoid data contamination from such faulty devices, it is important to incorporate devices with better stability and precision such as the ETM.

## 2 Technical description

The ETM can measure short or long ranges from ground calibration to geostationary target ranges at a PRF of up to 10 kHz or more and is ideal for SLR (Hamal et al. 1999). The ETM will time tag the start and stop epochs, associated with the "laser transmit" and "satellite receive" events, using independent channels. A TOF is then computed from such measurements by associating the correct events based on a priori knowledge of the expected ranges from the predictions. The SLR station instrumentation also collects raw data

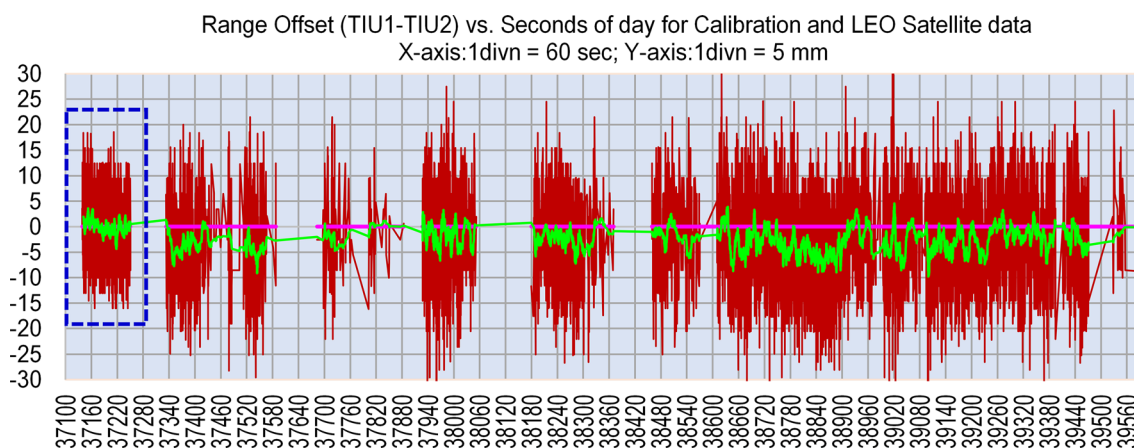


**Fig. 1** Shot by shot range differences of 2 TIUs vs. time of the day in seconds for LEO satellites. Red line shows shot by shot difference, green line is the 30-point MA, and the magenta line is the calibration

mean; blue dotted rectangle encloses the calibration data taken prior to the satellite data; X-axis: 1 divn = 60 s; Y-axis: 1 divn = 5 mm

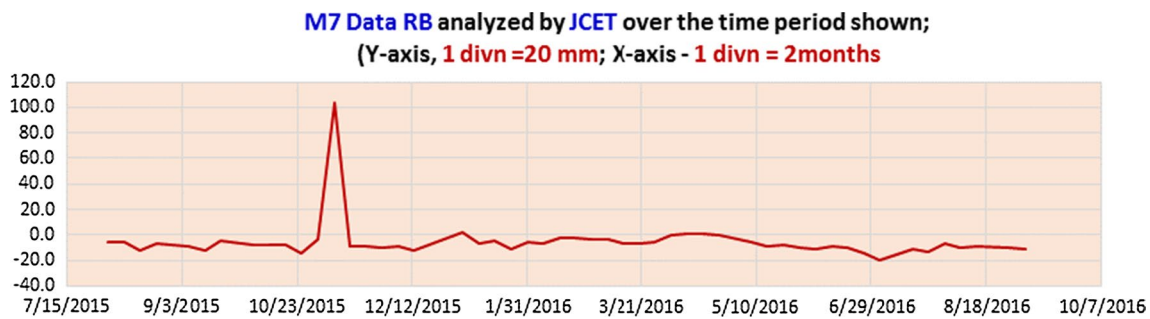


**Fig. 2** Example of a MOBLAS 7 (Greenbelt, 7105) jump in range bias (RB) of the TIU as seen in POD analysis; the plot shows range bias (in mm) on the Y-axis vs. Day of the Year (X-axis). The device was replaced after a few days and the station returned back to normal performance

on laser transmit/receive energies, telescope pointing angles, the meteorological data, the laser transmit epoch, and the time of flight (TOF). These data are acquired by the real-time control computer of the station every frame (variable from 100 to 250 ms depending on the satellite orbit) and is recorded in a raw data file. The raw data file is then processed by the Data Processing Computer (DPC) to compute the normal point (NP) as per the standard NP algorithm and processing criteria established by the ILRS ([https://ilrs.cddis.eosdis.nasa.gov/data\\_and\\_products/data/npt/npt\\_algorithm.html](https://ilrs.cddis.eosdis.nasa.gov/data_and_products/data/npt/npt_algorithm.html)). The DPC computes a trend function for the NP after fitting the residual range data with respect to the prediction, using medium- to high-order polynomial regression and iterative three-sigma filtering. The four statistical moments (viz., mean, standard deviation, skew, and kurtosis) are computed for the residual data (and therefore for the NP) to support the data QC. The resulting normal point data from each bin are transmitted to the NASA CDDIS and the European Data Center (EDC) for access by the international scientific community.

For the above NP computation, a full raw data file is required. Since the ETM data collected by its interfacing computer only have laser transmit epoch and TOF data, these data have to be synthetically integrated with the remaining instrument data for refraction correction, prior to computing the NP. An ETM-centric raw data file is created by swapping the epoch time and TOF of ETM data with the corresponding TIU raw data file upon completion of a data session, thus creating a frame by frame matching ETM raw data file similar to that of the TIU. This new process allows a concurrent scheme for data taking using the old (TIU) and new (ETM) hardware without inhibiting the operational data flow and without the need to put the station data in quarantine.

Cybioms Corporation manufactured the hardware and software for the 7 ETMs. These were extensively tested in its laboratory for a period of nearly 2 years for stability, precision, and range dependencies prior to incorporating into the NASA SLR network for station-based testing. Typical timing

stability observed in laboratory measurements was  $\sim 3$  ps with a calibration RMS of  $\sim 3$  ps. The test data were always taken with the same rigor as the operational data, and no changes were made to any of the hardware or software during this validation period. Initially, each of the 7 ETMs was tested for a period of 7 days at the MOBLAS 7 station for basic functional evaluation. This was not sufficient to provide a long-term comparison desired for geodetic measurements. Hence, several months of data collection were pursued subsequently to establish a substantial data set from the available LEO to GEO satellites at each of the stations. Unlike other similar work (Gibbs et al. 2002) of the past, the old (TIU) and new (ETM) hardware took simultaneous operational data at each of the stations to support direct shot by shot data comparison or normal point by normal point comparison by direct differencing without the need for any orbit analysis.

Figure 3 depicts a swap scheme that was designed for the multi-ETM intercomparison and a long-time (4–9 months) simultaneous data collection with a common TIU. This became necessary as we saw  $\sim -4$  mm systematic range bias (RB) in the data at MOBLAS 7 (M7, Greenbelt, MD, USA). Consequently, multiple (= 4) devices were compared sequentially to a common TIU at MOBLAS 7. All of these ETMs showed the same range bias at MOBLAS 7. An ETM device tested in MOBLAS 7 was then sent to MOBLAS 5 (M5, Yarragadee, Australia) for a 2-way intercomparison to legitimize the consistency of the observed range bias in MOBLAS 7. This two-station intercompared and cross-validated device was subsequently designated for MOBLAS 8 (M8, Tahiti), and the intercompared device at MOBLAS 7 was then sent to MOBLAS 4 (M4, Monument Peak, CA). Such intercompared and validated ETM devices in one or more stations were distributed in the network to have high confidence level in the comparison and observed range biases (if any). This provided a firm basis to apply any a posteriori fixed offset to correct the biased data.

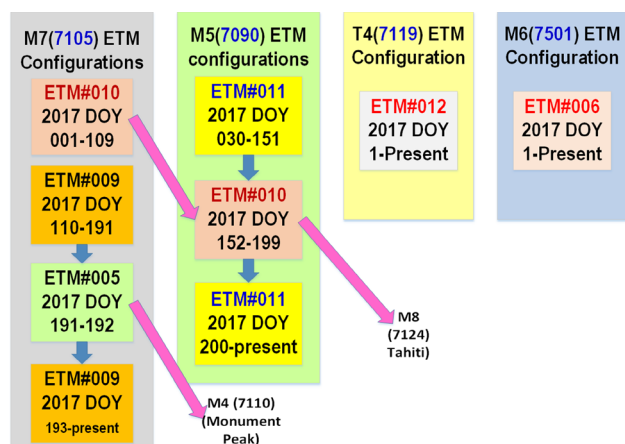


**Fig. 3** ETM interchanges made in MOBLAS 7 (Greenbelt, 7105) and MOBLAS 5 (Yarragadee, 7090) stations for intercomparison of the devices to determine the consistency of performance and to transition to the remaining stations

## 2.1 ETM: ground calibration and satellite performance

The ETMs have an internal calibration RMS of  $\sim 3$  ps and a ranging RMS of  $\sim 1$  mm ( $< 7$  ps) when simulating fixed ranges in the laboratory. In MOBLAS 7, these ETMs have generated a ground target single-shot RMS as small as 1.3 mm, a factor of 3 improvement over the corresponding TIU measurement. When the ranging system is performing optimally, the ETM ground target measurements yield submillimeter stability, which is  $\sim 3$ – $5$  times improvement over that of the TIU. LEO satellites, with a non-pulse broadening optical array, do support single-shot RMS of 2 to 4 mm with the ETM. In general, LEO passes (at 10 Hz operation) generate submillimeter normal points. The single-shot RMS of LAGEOS and GNSS satellites is limited by the photoelectron level of the satellite return as well as the retroreflector array spread function. The microchannel plate photomultiplier tube (MCP-PMT), operating in conjunction with a wide laser pulse width such as 150 ps and a pulse broadening satellite array, prevents substantial reduction in data RMS even with the ETM as the error is dominated by the rest of the data loop. Under fairly good acquisition and tracking conditions, the ETMs do generate submillimeter normal points even for LAGEOS.

## 2.2 ILRS data analysis for station qualification

As per the ILRS guidelines and practices, any data configuration change in an operational SLR station must go through quarantine followed by a rigorous data scrutiny by analysts. For any system data-related hardware upgrade, the ILRS has a minimum requirement of 20 LAGEOS and

LAGEOS 2 passes along with 20 LARES satellite passes for QC analyses by the Analysis Standing Committee (ASC) (Otsubo et al. 2018). The NASA Space Geodesy Project (SGP) (Merkowitz et al. 2018) has established a more stringent longer duration (six or more months) testing, and the concurrent data generation capability easily supported such a long-term data comparison with no impact on the operational data. During the data gathering phase, the engineering analysis was performed periodically by Cybioms, using the full rate and the NP data. The entire NP data from the stations was subsequently supplied by the operations group at Peraton, as quarantined data to CDDIS, for further analysis and validation by JCET.

## 2.3 MOBLAS 7 short-term data analysis and results

The short-term (1 hour (h)) system ranging stability is an important performance metric for a SLR system. This test is performed on accurately ( $\sim 1$  mm) surveyed ground targets using thousand-point data files taken continuously for a period of 1 h. The ETM generated submillimeter ( $< 0.5$  mm) peak-to-peak variations with an RMS of  $\sim 1.7$  mm for the 1-hour stability, while the TIU produced  $\sim 2$  mm variations with a RMS of  $\sim 3.8$  mm for the same set of events. This observed field performance was consistent with the laboratory data, where temperature can be maintained tightly. When the data are taken within the dynamic range ( $< 8$ ) of the discriminator, submillimeter stability was consistently obtained for the ETM. Care is taken to confine the data taking to the linear dynamic range of the discriminator. Although this is possible for calibration, it is nearly impossible to consistently constrain the satellite data to the linear range due to the stochastic nature of the laser propagation through the atmosphere as well as the coherent nature of reflection from the satellite optical array. When it is outside of the dynamic range, the nonlinearity of the signal processing electronics will alias the data resulting in a larger RB and normal point precision.

Figure 4 illustrates the TIU–ETM comparison on LEO, MEO, and HEO satellites for a 3-month comparison. Here, the orbit analysis is not used; instead, a direct comparison of the shot by shot ranges was used. There are no major systematic variations or trends except for a fixed consistent offset for all satellite groups. For the intercomparison of the ETM and the TIU performance on satellites, the raw simultaneous data as well as the individual normal point data were used. The composite mean and RMS of each group of data were then computed. If the linear regression of the difference data shows no slope or variations, then this indicates a stable intercomparison result. As can be seen in Fig. 4, each of the satellite groups (LEO, LAGEOS, and HEO) exhibited range biases from  $-4.3$  to  $-4.4$  mm for MOBLAS 7. This observed RB was a significantly large one, and hence, NASA

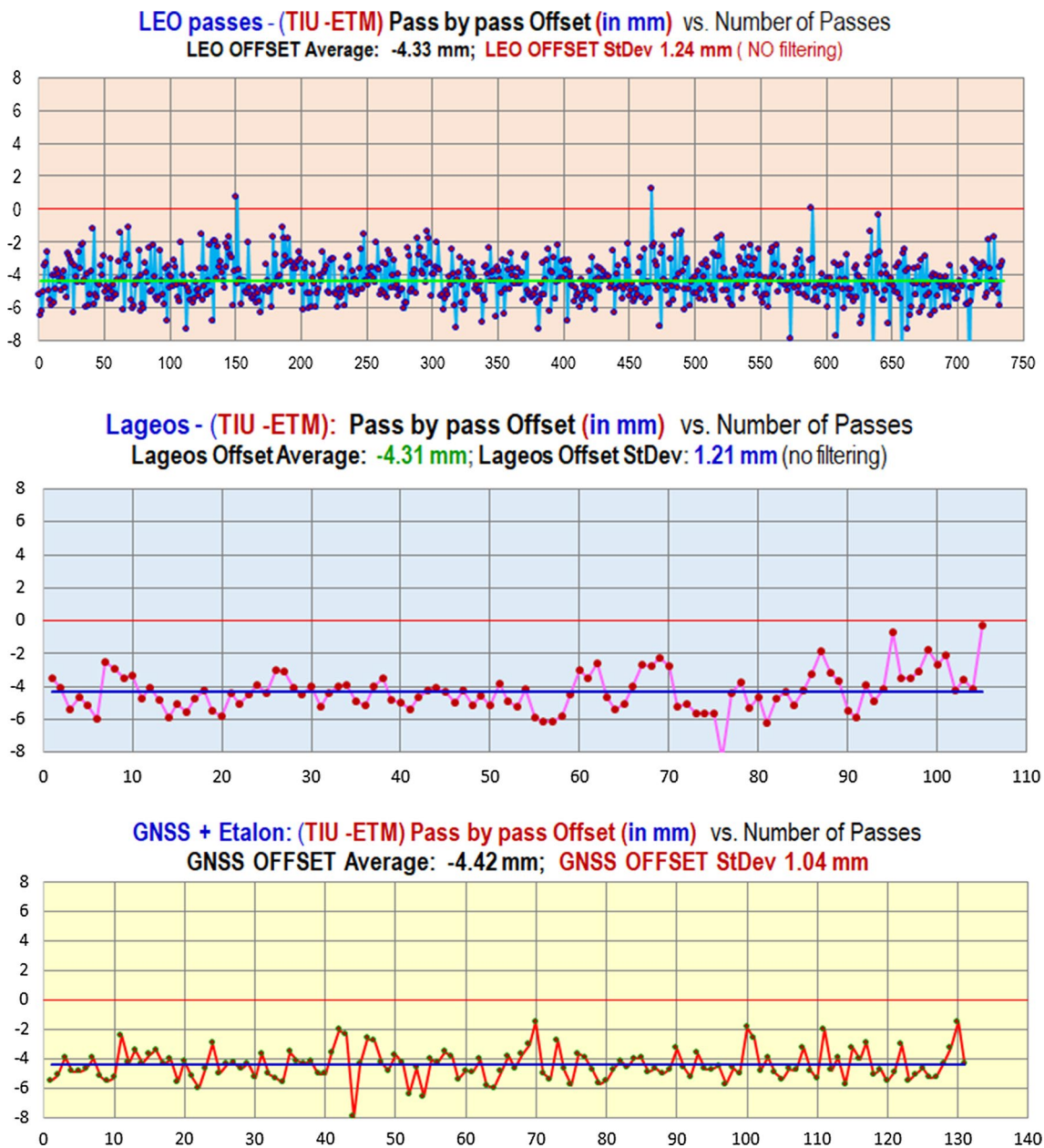


**Fig. 4** Mean of the MOBLAS 7 (7105) range differences (i.e., TIU-ETM) computed from the raw time of flight data for each pass vs. the Number of the pass (X-axis). The tracked passes include LEO, MEO, and HEO satellites. These 3-month data depict every pass collected during this period, and the mean offset is ~-4 mm with an

RMS of ~1 mm for each satellite group. No iterative 3-sigma filtering was performed for computing the above mean offset. Y-axis, 1 divn = 2 mm. X-axis scale depicts the pass number, and the scale varies depending on the plot.

SLR program needed further corroboration with other ETM devices. Similar results were obtained in 4 other comparisons with 4 different ETMs while using the same TIU. The ETMs tested at MOBLAS 7 that showed a consistent difference of ~-4 mm with the TIU, when tested in MOBLAS 5, showed only sub-mm difference with the MOBLAS 5 TIU, thus corroborating the source of the problem to be the MOBLAS 7 TIU. The fairly constant range bias seen in

all satellite groups in MOBLAS 7 suggests that there is a problem for the TIU in its measurement of the calibration range. This problem appears to be uniquely present in the MOBLAS 7 TIU only and not in the ones installed in the rest of the NASA stations. It so happens that this offset is consistent with the RB seen by the analysts over a period of 2 years, thus confirming the root cause of the RB problem (Fig. 5). There was a similar finding (Selden et al. 1992) for

the HP 5370B counter, when 2 TIUs were compared and also in Stanford counters (Gibbs et al. 2002).

## 2.4 MOB-LAS 7 long-term data analysis and results

The ETM was established as the operational device in MOB-LAS 7 in July 2016. The residual data for the MOB-LAS 7 station at Greenbelt (7105) from the LAGEOS orbit, computed by JCET for a five-year period of Sep 2013 through Aug 2018, are shown in Figs. 5 and 6. Figure 5 represents the TIU data for the first 3 years of this period, while Fig. 6 shows the ETM performance for the last 2 years of this period. The 3-sigma filtered values of the ETM- and

TIU-based SLR residual data are shown in the histograms in Fig. 7. The mean RB offset between the two groups of data in Figs. 5 and 6 shows a mean difference of  $\sim -3$  mm with a near-Gaussian distribution. This matches the range offset measured between the 2 devices, indicating that the older TIU had a RB of comparable value and the new ETM is practically immune from it. The ETM data show less RB with respect to the orbit and are closer to the zero mean bias than the TIU. There is skewness in the histograms of both groups of data, but looks similar, possibly arising from the dependencies on other parts of the data hardware or fitting models, applied corrections, etc.

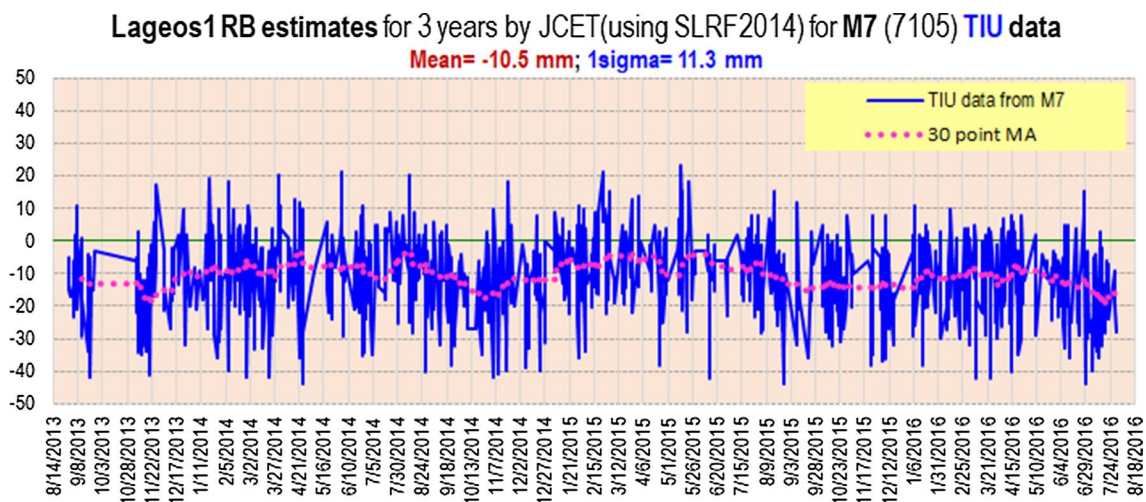


**Fig. 5** TIU-based RB estimates for MOB-LAS 7 (7105) LAGEOS 1 data with respect to a global SLR orbital fit for a period of 3 years from Aug 2013 to Jul 2016; Y-axis scale: 1 division (divn) = 10 mm; X-axis scale 1 divn = 25 days)

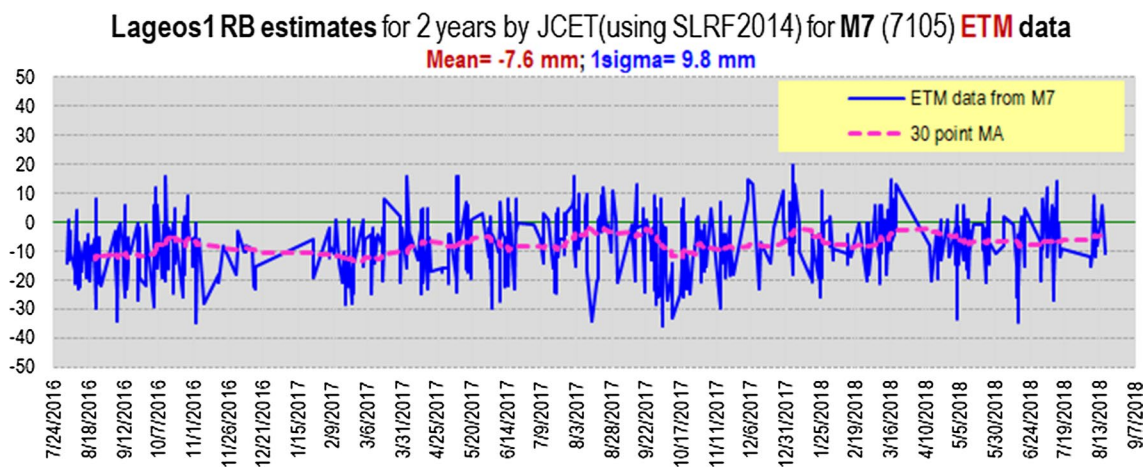
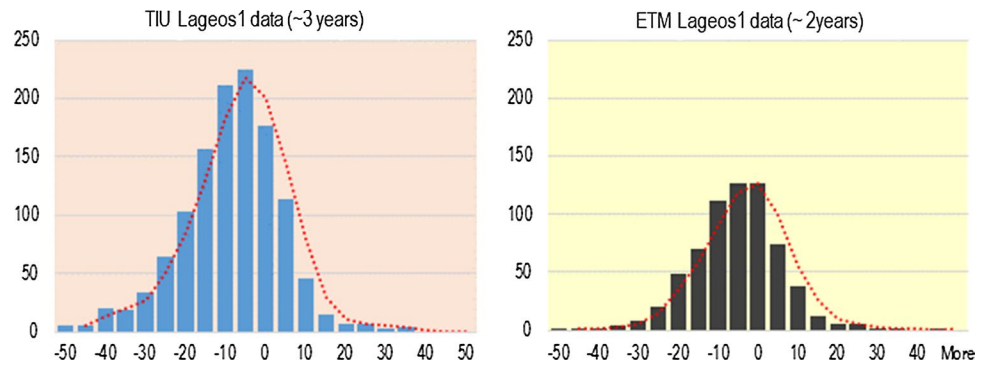


**Fig. 6** ETM-based RB estimates for MOB-LAS 7 (7105) LAGEOS 1 data with respect to a global SLR orbital fit for a period of 2 years from Aug 2016 to Aug 2018 (X-axis). The differences in the mag-

nitude of the RB offset and the 1 sigma values are explicitly clear when compared to Fig. 5. Y-axis scale: 1 divn = 10 mm; X-axis scale 1 divn = 25 days)

**Fig. 7** Histograms and statistics of the residuals (in mm) for MOBLAS 7 (7105) LAGEOS data shown in Figs. 5 and 6. The differences in the offset and the skewness are shown



### 2.5 MOBLAS 5 (Yarragadee, 7090) short-term and long-term analysis results

Extensive testing and analysis of the ETM performance were also performed for MOBLAS 5 (Yarragadee, 7090) similar to the tests at MOBLAS 7 (Greenbelt, 7105). In this case, we had a much larger data set comprising of ~ 120,000 normal points covering LEO to GEO satellites. In the MOBLAS 7 comparison studies, we did not have any GEO satellites in the mix since no GEO satellites are visible from that geographic location. We also had a much smaller HEO data set, especially for daytime conditions. Figure 8 illustrates the difference for the LAGEOS 1 and 2 data sets for the two ETM devices (shown in blue and red) for a period of ~6 months, with each group of data processed with its own 3-sigma filter. The respective mean values are also shown by straight lines along with its statistics. As can be seen, the offset difference between the two groups of data is very small (<0.2 mm), with very close sigma values indicating the consistency of the ETMs-TIU intercomparison.

Table 1 is a summary of the analysis of the data groups that were used for this detailed comparison of TIU and ETM ranges. “Allsat” is an aggregation of all satellite data sets into a single group for data processing and common filtering. This type of aggregation and combined analysis is possible since various satellite data groups show sub-mm difference in the mean range offset between them, and data aggregation does not lend itself to any significant shift from the individual observed biases.

Table 2 highlights the intercomparison of the ETM data groups (ETM#010 and ETM#011) in MOBLAS 5 against the same TIU. The consistency between the two ETMs is explicitly clear from the sub-mm agreement shown in the third column of Table 2. Each group of difference data, based on the Day of the Year (DOY) and the device used, has significant amount of data yielding a robust mean with a small 1-sigma value. This gives further credence to the consistent behavior of the different ETM instruments, which is what is desired for a bias-free network. Unlike the TIUs, the ETMs show picosecond-level (sub-mm) linearity and stability from calibration to satellite ranges,

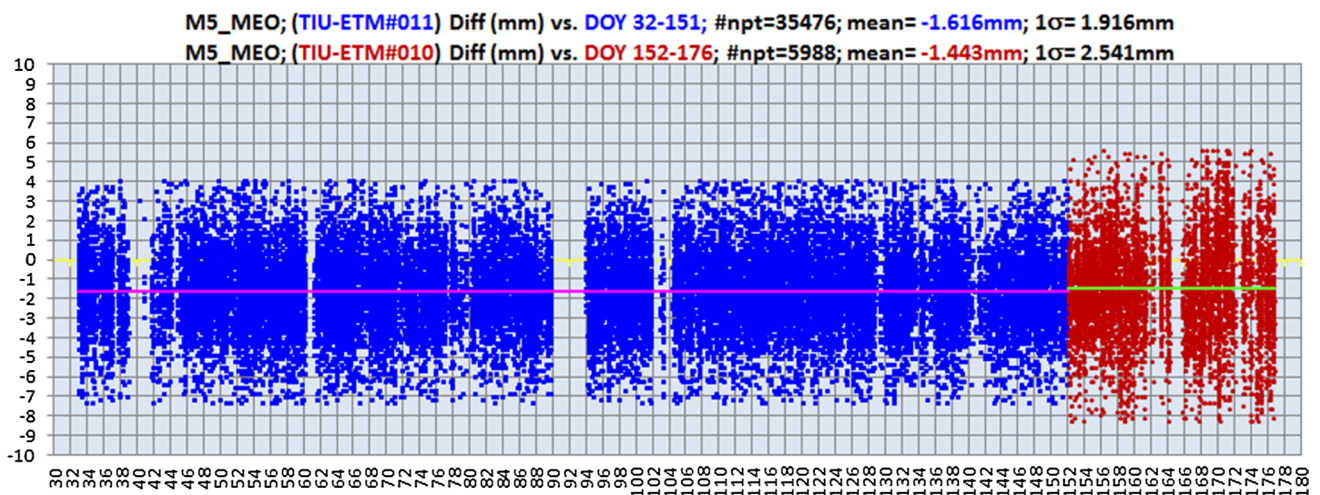


**Fig. 8** M5 (7110) LAGEOS 1 and 2 data normal point differences between TIU and ETM vs. Day of the Year (DOY). The mean offset and 1-sigma values for each group of data are shown for the two different ETMs. (Y-axis, 1 divn = 1 mm; X-axis, 1 divn = 2 days)

thus minimizing instrument-related systematic measurement errors for time of flight. Figure 9 illustrates the trend from the MOBLAS 5 long-term operational data analysis for the TIU and ETM. As it can be seen, the ETM-based

operational data show tighter dispersion than a comparable period of 1 year operated by the TIU.

The benchmarked MOBLAS 7 ETM that was sent to MOBLAS 4 was used for collecting data at that station over

**Table 1** MOBLAS 5 Range intercomparison summary for LEO to GEO satellites

M5: TIU and ETM SLR data comparison for data groups based on Day of the Year (DOY) and satellite orbit	Mean of TIU-ETM range offsets	1 sigma (mm)
M5-2017_DOY 32-176_Allsat files (using ETM-010 and ETM-011)	-1.32	2.32
M5-2017_DOY 32-176_LEO files (using ETM-010 and ETM-011)	-1.55	2.24
M5-2017_DOY 32-176_MEO files (using ETM-010 and ETM-011)	-1.59	2.01
M5-2017_DOY 32-176_HEO files (using ETM-010 and ETM-011)	0.86	2.29
M5-2017_DOY 32-176_GEO files (using ETM-010 and ETM-011)	0.90	3.10
Grouping based on the ETM device used		
MS-2017_DOY 032-151_Allsat files (using ETM-011)	-1.33	2.20
MS-2017_DOY 152-176_Allsat files (using ETM-010)	-1.22	2.72

**Table 2** MOBLAS 5 Range Intercomparison summary for different ETMs and for data groups from LEO to GEO

M5—Paired Data between the TIU and ETM#011 and ETM#010 based on dates (DOY) of deployment	Mean offset between the TIU and ETM* (mm)	Delta between the pairs based on the satellite orbit (mm)	St.Dev (mm)	Number of normal points
M5-TIU-ETM-2017-npt-diff - DOY032-151 (GEO 1)	0.46	0.19	2.52	1162
M5-TIU-ETM-2017-npt-diff - DOY152-176 (GEO 2)	0.65		2.64	311
M5-TIU-ETM-2017-npt-diff - DOY032-151 (HEO 1)	0.70	0.05	1.94	9481
M5-TIU-ETM-2017-npt-diff - DOY152-176 (HEO 2)	0.75		2.45	2146
M5-TIU-ETM-2017-npt-diff - DOY032-151 (MEO 1)	-1.62	0.17	1.92	35,476
M5-TIU-ETM-2017-npt-diff - DOY152-176 (MEO 2)	-1.44		2.54	5988
M5-TIU-ETM-2017-npt-diff - DOY032-151 (LEO 1)	-1.56	0.05	2.09	56,478
M5-TIU-ETM-2017-npt-diff - DOY152-176 (LEO 2)	-1.51		2.68	11,620

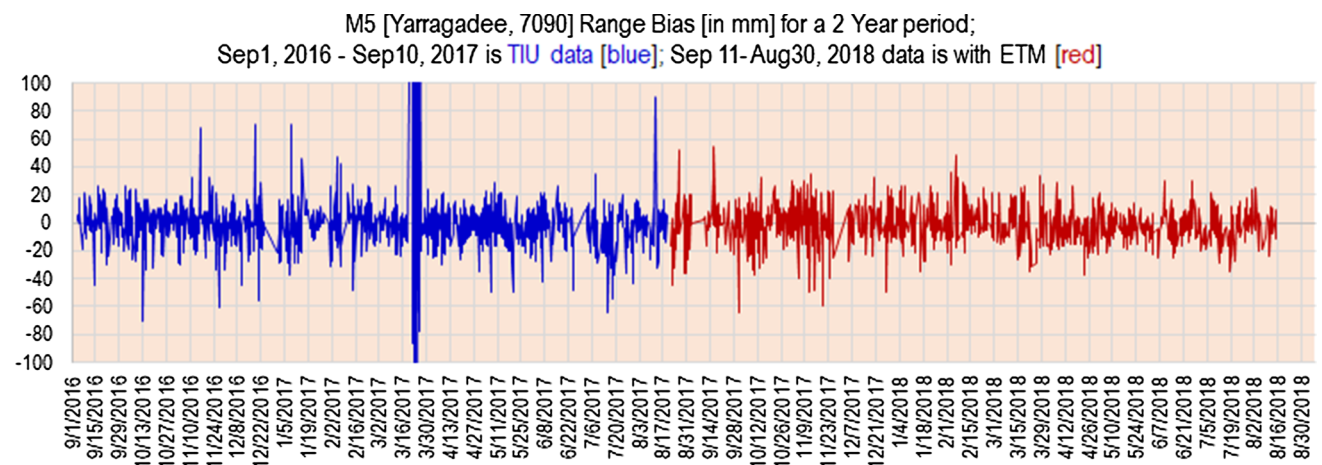


**Fig. 9** M5 (7090) long-term RB analysis for LAGEOS 1 based on the operational periods of the TIU and ETM. The ETM was made as the operational device in August 2017. The Y-axis depicts the RB in mm,

while the X-axis covers the 2-year period with each division corresponding to 14 days

a period of nearly 10 months. The data taken there by direct differencing of the TIU and ETM showed submillimeter consistency for the mean value for the normal point differences for the various satellite groups. There has been a reported geodetic bias of  $\sim 10$  mm at the MOBBLAS 4 station starting 2010, and the intercomparison between the TIU and ETM showed that the RB problem is outside of the station time of flight measurement electronics.

## 2.6 Direct NP range comparisons

The ILRS AC hosted at JCET is one of the ACs responsible for the QC analysis of station changes and upgrades. The process of the TIU replacement by ETMs was one of the areas that JCET is involved in comparing directly the ranges collected at each of the sites with the two different technologies simultaneously. Depending on the site, different amounts of ranging data were supplied by the NASA Network, covering different groups of targets, primarily dependent on the capabilities of the tracking system. Nevertheless, a wide range of orbital altitudes from tens of different missions was involved for all systems. In each case, the data were first processed to identify the pair of corresponding ranges which were recorded simultaneously by both technologies, the TIU and the ETM. Once this was completed, the differences and their statistics were formed for each target and in the last step, and the weighted mean of the mean differences was formed along with its standard deviation. The results are summarized in Table 3 arranged in groups of orbital regimes and as a weighted average based on all entries for each site. This type of direct comparison does not involve any orbital analysis, and no modeling assumptions are required whatsoever. As it can be seen, these results as all previous ones identified only one case where a significant difference exists between the two sets of data (TIU and ETM). This is the case of Greenbelt, 7105 (MOBBLAS 7), with a bias of  $-4.05 \pm 0.40$  mm. This will be further investigated and a correction to all data prior to switching to the ETM technology, affected by this bias, will be corrected in subsequent reanalysis for the ILRS contribution to the ITRF. This result corroborates the statistically identical result that was seen in the standard QC processing of the two data sets that identified a bias of the same magnitude. Quantifying such errors at each site is very important because it helps explain and rationalize the observed variations in the systematic error characterization of these systems as they are estimated from long-term data analysis of the network (Appleby et al. 2016; Luceri et al. 2019).

## 3 Conclusions

The introduction of the event timers in the NASA SLR network has allowed the network transition to a modern, highly precise time measurement technique with picosecond stability and precision while allowing the network to baseline its range biases. ETMs, on the average, reduced the calibration data single-shot RMS to less than 2 mm, a factor of 2 improvement, while improving the calibration stability by a factor of 2 to 5 to sub-mm. SLR operations at 10 Hz to LEO satellites and LAGEOS have produced submillimeter normal points under fairly good tracking conditions. The short-term and long-term ranging performance improvement was pursued successfully by identifying and reducing the systematics in the network stations. In this regard, the long-term (6–12 months) characterization and validation of the ETM devices in an operational setting were accomplished by the newly established concurrent data-taking approach of the old (TIU) and new (ETM) hardware. This scheme allowed the operational TIU configuration to remain unperturbed while enabling the inclusion and comparison of multiple ETM devices. The station-specific and orbit-dependent range biases of the TOF electronics were uncovered at the millimeter level using the global orbit fit as well as the direct comparison of the ranges, leading the way to establish the systematic biases and improve space geodetic data and products. The RB seen at MOBBLAS 7 to the tune of  $-4$  mm evaded prior efforts to uncover and this upgrade pinpointed the problem solely to the time of flight measurement device used, viz., the TIU. Equally, the RB seen by analysts in MOBBLAS 4 was verified to be outside of the station data loop hardware. The technical approach of intercomparing and benchmarking the ETM devices and then transferring this to other network stations allowed the in situ multi-station comparison and normalization at the millimeter level. The multi-ETM intercomparison and the ETM transfer among the stations of the NASA SLR network successfully standardized the critical time of flight measurement electronics across the entire network. To the best of our knowledge, there has never been such an exhaustive long-term (years) effort among the ILRS stations to intercompare the data hardware at the multi-station level to deduce millimeter-level performance. This has allowed NASA to uniquely implement the benchmarked and cross-normalized hardware across the NASA SLR network in its quest to harmonize the operations toward the space geodetic millimeter goal.

**Table 3** Summary of the results from the direct comparison of the six NASA sites that provided concurrent data taken with the standard TIU and the ETM technology systems

Site	ILRS ID#	Orbital Regime	Mean $\Delta\rho$ (mm)	Std. Dev. (mm)	No. of events	Missions Providing Data
Monument Peak, CA, USA	7110	LEO	0.14	0.53	10,395	
Monument Peak, CA, USA	7110	MEO	0.17	1.10	6278	
Monument Peak, CA, USA	7110	HEO	0.21	0.54	305	
Monument Peak, CA, USA	7110	<b>ALL</b>	<b>0.17</b>	<b>0.36</b>	<b>17,023</b>	<b>25</b>
Yarragadee, Australia (ETM10)	7090	LEO	-1.62	0.82	11,837	
Yarragadee, Australia (ETM10)	7090	MEO	-1.49	1.16	6163	
Yarragadee, Australia (ETM10)	7090	HEO	1.20	0.56	2409	
Yarragadee, Australia (ETM10)	7090	GEO	0.56	2.21	149	
Yarragadee, Australia (ETM10)	7090	<b>ALL</b>	<b>0.08</b>	<b>0.42</b>	<b>20,558</b>	<b>60</b>
Yarragadee, Australia (ETM11)	7090	LEO	-1.43	0.63	7582	
Yarragadee, Australia (ETM11)	7090	MEO	-1.63	0.93	4992	
Yarragadee, Australia (ETM11)	7090	HEO	0.92	0.48	1415	
Yarragadee, Australia (ETM11)	7090	GEO	0.16	3.51	49	
Yarragadee, Australia (ETM11)	7090	<b>ALL</b>	<b>-0.17</b>	<b>0.35</b>	<b>14,038</b>	<b>50</b>
Hartebeesthoek, South Africa	7501	LEO	0.29	0.79	10,790	
Hartebeesthoek, South Africa	7501	MEO	0.33	1.43	8650	
Hartebeesthoek, South Africa	7501	HEO	-0.50	0.68	1692	
Hartebeesthoek, South Africa	7501	<b>ALL</b>	<b>-0.09</b>	<b>0.49</b>	<b>21,132</b>	<b>46</b>
Greenbelt, MD, USA (ETM10)	7105	LEO	-3.93	0.52	539	
Greenbelt, MD, USA (ETM10)	7105	MEO	-8.20	1.00	402	
Greenbelt, MD, USA (ETM10)	7105	HEO	-4.98	0.78	40	
Greenbelt, MD, USA (ETM10)	7105	<b>ALL</b>	<b>-4.05</b>	<b>0.40</b>	<b>981</b>	<b>29</b>
Tahiti, French Polynesia	7124	-	-	-	-	-
Arequipa, Peru	7403	LEO	0.32	0.95	6809	
Arequipa, Peru	7403	MEO	0.11	1.87	2759	
Arequipa, Peru	7403	<b>ALL</b>	<b>0.28</b>	<b>0.85</b>	<b>9568</b>	<b>24</b>
Haleakala, HI, USA	7119	LEO	-0.32	0.85	8518	
Haleakala, HI, USA	7119	MEO	0.05	1.23	7871	
Haleakala, HI, USA	7119	<b>ALL</b>	<b>-0.20</b>	<b>0.70</b>	<b>16,389</b>	<b>23</b>

Bold values indicates the combined statistics of all satellite groups

Orbital height LEO:  $h_o < 1000$  km

Orbital height MEO:  $1000 \text{ km} \leq h_o < 6000$  km

Orbital height HEO:  $6000 \text{ km} \leq h_o < 25,000$  km

Orbital height GEO:  $25,000 \text{ km} \leq h_o$

**Acknowledgements** The authors wish to acknowledge the SLR operations program management at NASA codes 453 and 61A and the SLR network operations team at the OC and the NASA field stations. E. C. Pavlis and M. Kuzmich-Cieslak acknowledge the support of NASA Grant NNX15AT34A. We thank the referees for their reviews and many helpful comments.

**Author Contributions** TV manufactured the ETMs, developed the software approach for integration into the NASA stations, integrated and tested the hardware and software in the laboratory, installed and tested the ETMs in the NASA stations, analyzed the data, and wrote the paper, RLR developed the ETM software and the integration software for ETM normal point processing on the Data Processing Computer, ECP performed data analysis from the AC perspective and provided contributions for the article including review, MK-C performed data analysis

from the AC perspective, and SMM performed the article review and provided project leadership. DAS (1) Bulk of the data is in the NASA CDDIS and NASA SLR station archives (90%); <https://cddis.nasa.gov>. (2) University of Maryland Baltimore county JCET (9%) <http://geode.sj.cet.umbc.edu/QC/>. (3) Cybioms Corporation (1%) - NO web link, manufacturer data.

## References

Altamimi Z, Rebischung P, Metivier L, Collilieux X (2016) ITRF2014: a new release of the international terrestrial reference frame modeling nonlinear station motions. *J Geophys Res Solid Earth*. <https://doi.org/10.1002/2016JB013098>

- Appleby G, Rodríguez J, Altamimi Z (2016) Assessment of the accuracy of global geodetic satellite laser ranging observations and estimated impact on ITRF scale: estimation of systematic errors in LAGEOS observations 1993–2014. *J Geod* 90:1371. <https://doi.org/10.1007/s00190-016-0929-2>
- Arnold D, Montenbruck O, Hackel S et al (2018) Satellite laser ranging to low Earth orbiters: orbit and network validation. *J Geod*. <https://doi.org/10.1007/s00190-018-1140-4>
- Gibbs P, Appleby G, Potter C (2002) A reassessment of laser ranging accuracy at SGF Herstmonceux, UK. [https://cddis.nasa.gov/lw13/docs/presentations/time\\_gibbs\\_1p.pdf](https://cddis.nasa.gov/lw13/docs/presentations/time_gibbs_1p.pdf)
- Hamal K, Prochazka I, Blazej J (1999) Contribution of the pico event timer to satellite laser station performance improvement. In: *Laser radar ranging and atmospheric lidar techniques II*. International Society for Optics and Photonics, p 38–42
- Luceri V, Pirri M, Rodríguez J, Appleby G, Pavlis EC, Müller H (2019) Systematic errors in SLR data and their impact on the ILRS products. *J Geod*. <https://doi.org/10.1007/s00190-019-01319-w> (**this issue**)
- McGarry JF, Hoffman ED, Degnan JJ et al (2018) NASA's satellite laser ranging systems for the twenty-first century. *J Geod*. <https://doi.org/10.1007/s00190-018-1191-6>
- Merkowitz SM, Bolotin S, Elosegui P et al (2018) Modernizing and expanding the NASA space geodesy network to meet future geodetic requirements. *J Geod*. <https://doi.org/10.1007/s00190-018-1204-5> (**this issue**)
- Otsubo T, Müller H, Pavlis EC et al (2018) Rapid response quality control service for the laser ranging tracking network. *J Geod*. <https://doi.org/10.1007/s00190-018-1197-0> (**this issue**)
- Pearlman M, Arnold D, Davis M et al (2019) Laser geodetic satellites: a high-accuracy scientific tool. *J Geod*. <https://doi.org/10.1007/s00190-019-01228-y>
- Selden M, Varghese T, Heinick M, Oldham T (1992) Proceedings of the SLR workshop. *ilrw8\_section04*, PP 4-1 through 4-8